Theor Chem Acc (2010) 125:493–501
DOI 10.1007/s00214-009-0662-5

REGULAR ARTICLE

Application of the elongation method to the electronic structure of spin-polarized molecular wire under electric field

Yuuichi Orimoto · Feng Long Gu · Jacek Korchowiec · Akira Imamura · Yuriko Aoki

Received: 27 January 2009 / Accepted: 15 October 2009 / Published online: 5 November 2009

Abstract The elongation method has been applied to elucidate the spin-dependent behavior of the pyrrole-based spin-polarized molecular wire containing 1-pyrrolylphenyl nitronyl nitroxide with oligothiophene units under the influence of an applied electric field. It was found that the donor pyrrole ring causes the delocalization of electrons over the molecular wire regardless of the spin-orientation. In addition, nitronyl nitroxide as a radical unit shows two important features. First, it changes the spin-distribution of the delocalized electrons from same ratio of α- and β-spins to dominant β-spin. Second, it shifts the distribution of electrons in the same direction as that of the applied electric field.

Keywords Elongation method · Spin-polarized molecular wire · Spin-polarized donor · 1-Pyrrolylphenyl nitronyl nitroxide · Electric field · Electronic structure

Dedicated to Professor Sándor Suhai on the occasion of his 65th birthday and published as part of the Suhai Festschrift Issue.

Y. Orimoto · F. L. Gu · J. Korchowiec · Y. Aoki
Department of Material Sciences, Faculty of Engineering Sciences, Kyushu University, 6-1 Kasuga-Park, Fukuoka 816-8580, Japan

A. Imamura
Hiroshima Kokusai Gakuin University, 6-20-1 Nakano, Aki-ku, Hiroshima 739-0321, Japan

Y. Aoki (✉)
Japan Science and Technology Agency, CREST, 4-1-8 Hon-chou, Kawaguchi, Saitama 332-0012, Japan
e-mail: aoki@mm.kyushu-u.ac.jp

Present Address:
F. L. Gu
Center for Computational Quantum Chemistry, South China Normal University, Guangzhou 510631, China

Present Address:
J. Korchowiec
K. Gumiński Department of Theoretical Chemistry, Jagiellonian University, R. Ingardena 3, 30-060 Kraków, Poland

1 Introduction

In recent years, spin-dependent transport such as spin valve, etc., has drawn considerable interest in the field of spin electronics for the applications to magnetic information storage [1–7]. In the spin valve, a non-ferromagnetic material is inserted between two electrodes of ferromagnetic half-metals [8] in which the Fermi level crosses only one side of the spin-band. Spin-polarized electrons that are induced by the potential difference can be transported through the non-ferromagnetic material without losing the spin-information. As an alternative approach to control the spin-information, an intramolecular spin alignment in π-conjugated organic systems has been investigated for "molecular magnetism" [9–24]. In such systems, the spin-information is transmitted through π-electron network.

More recently, quantum wires such as spin-polarized molecular wire [25–28] or spin-polarized nano wire [29] were designed for controlling the electronic spins in the wires. In particular, spin-polarized molecular wire **1**, as shown in Fig. 1a, has been the subject of considerable attention as a new type of spin-rectifying molecular system [25]. Pyrrole-based spin-polarized molecular wire **1** consists of two parts, that is, spin-polarized donor (SPD) [22–24, 30–38] and molecular wire. The SPD part is a pyrrole-based SPD **2**, 1-pyrrolylphenyl nitronyl nitroxide,

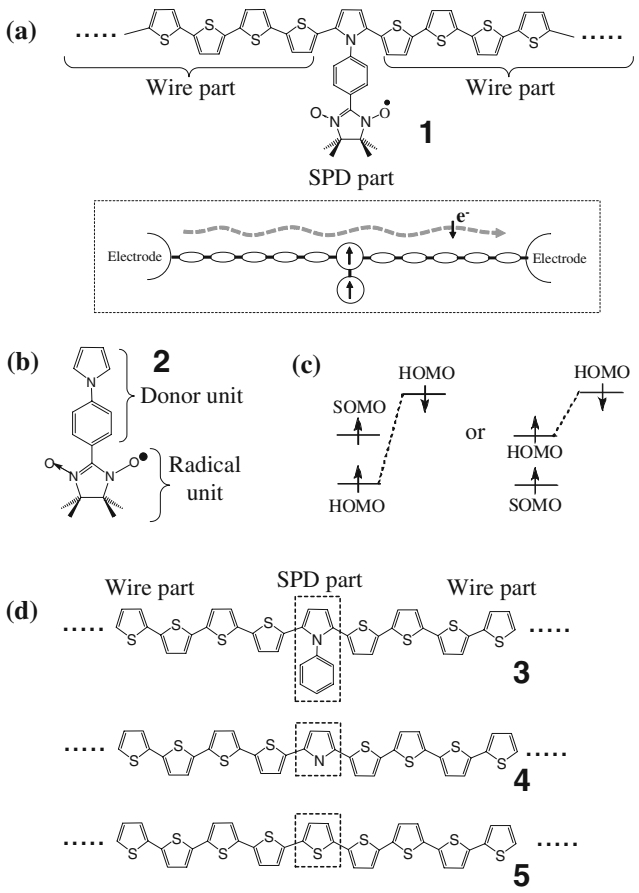

Fig. 1 **a** Geometries of pyrrole-based spin-polarized molecular wire **1**. **b** Geometry of spin-polarized donor (*SPD*) (1-pyrrolylphenyl nitronyl nitroxide) **2**. **c** Properties of molecular orbitals for spin-polarized donor. **d** Model molecules for the pyrrole-based spin-polarized molecular wire. "SPD part" is indicated by *boxes* in broken line. The other region was defined as "wire part"

as shown in panel (b) of Fig. 1. In addition, the SPD part can be further divided into two units, electron-releasing "donor unit" that includes pyrrole and phenyl rings, and "radical unit" composed of a nitronyl nitroxide (NN). Oligothiophene chains construct the wire part. Due to the unpaired electron in the central SPD part, the whole system **1** retains doublet state.

At the unrestricted Hartree–Fock (UHF) level of theory, SPD molecule **2** has three important spin orbitals (Fig. 1c): a singly occupied α-spin orbital "SOMO(α)", the highest doubly occupied α-spin orbital "HOMO(α)", and its β counterpart "HOMO(β)". The most important feature of the SPD molecule is that the orbital energy of HOMO(β) is higher than that of SOMO(α). For instance, semi-empirical UHF calculations predicted the higher energy HOMO(β) in NN derivatives [33–36]. This can be explained by spin polarization effects and the increases in energy of the HOMOs due to the electron-releasing donor effects. This is in contrast to the property of general radical molecules in doublet state, where the orbital energy of SOMO(α) is higher than that of HOMO(β).

It was expected by experimentalists that in the spin-polarized molecular wire, the β-spin electron of SPD part can be removed under the applied electric field corresponding to a primary oxidation potential along the wire [25] (see the bottom of Fig. 1a). The first oxidation, removal of β-spin electron from the HOMO(β), changes the multiplicity of the system from doublet to triplet state. The triplet state is expected by considering the exchange interactions due to a non-disjoint type linkage between donor and radical units. In fact, the triplet ground state of SPD molecule **2** after one-electron oxidation was observed experimentally [36]. The triplet ground state of mono-cationic SPD molecule **2** was examined at the several levels of theory for the geometry optimized under the constraint of planarity (see Table 1). Our calculations predicted the triplet ground state at both the spin-projected UHF/6-31G(d) and UPM3 levels, while UB3PW91/6-31G(d) shows the singlet ground state. The current through the molecular wire is spin polarized to β-spins in the triplet state because the unoccupied β-orbital after removal of an electron can be used for transporting β-electrons. In the next step, an α-electron will be removed by the applied electric field corresponding to a secondary oxidation potential, and the system returns to the doublet state. In contrast to the triplet state, an α-spin current passes through the wire part, because the unoccupied α-orbital after the removal is used for transporting α-electrons. Therefore, this system has a potential for rectifying the type of electron spins of tunneling current through the molecular wire.

Theoretical studies have been actively conducted on the properties of molecular wires [29, 39–46], for example, spin filtering properties of sandwich molecular wires [45, 46], charge transport properties of molecular semiconductors under an external electric field [41]. However, little is known about the electronic structure of spin-polarized molecular wire **1** and its behavior in an applied electric field.

The elongation method [47–59] was developed to efficiently determine the electronic structures of quasi-one dimensional periodic and non-periodic polymers. This method mimics the mechanism of the experimental

Table 1 Total energy difference (in a.u.) between singlet and triplet states for mono-cationic pyrrole-based spin-polarized donor **2**

Calculation level	Total energy (in a.u.) Triplet–singlet
PUHF/6-31G(d)	−0.08998
UB3PW91/6-31G(d)	0.01306
UPM3	−0.00877
UPM3//PUHF/6-31G(d)	−0.01971

polymerization. Monomer units attack a starting cluster step by step, therefore the electronic states can be determined when the system is elongated. In this article, we applied the UHF variant of the elongation method (UHF-elongation) to the spin-polarized molecular wire that retains a radical electron.

The purpose of the present article is to elucidate the electronic structure of the spin-polarized molecular wire **1** in the presence of an electric field using the elongation method. The paper is organized as follows. In Sect. 2, we briefly review the elongation method at the UHF level of theory. In Sect. 3.1, the electronic structure of SPD molecule **2** is analyzed. In Sects. 3.2 and 3.3, the elongation method is applied to calculate the electronic states of the spin-polarized molecular wire in an electric field. Finally, the conclusions are given in Sect. 4.

2 Method

In this section, we will briefly describe the elongation method using the spin-polarized molecular wire **1** as an example. The whole elongation procedure can be summarized as follows (see also Fig. 2):

(a) A starting cluster includes the central SPD part and eight thiophene rings, four at each side of the SPD part. The elongation calculations are initialized by conventional UHF method under the applied electric field, $\vec{E}$. The size of the starting cluster, N_{st}, is the number of thiophene rings. $N_{st} = 8$ is used in the current elongation run.

(b) The canonical molecular orbitals (CMOs) of the starting cluster are converted to localized MOs (LMOs) by a unitary transformation. Two distinct sets of LMOs are obtained. One contains the LMOs which are assigned to the frozen region. The other set is assigned to the active regions. The frozen region, denoted as A, is the central SPD part, while the active regions, denoted as B, are the thiophene rings attached to both sides of the SPD. In the next step, two new thiophene rings, let us say C-monomers, attack both sides of the B regions. The frozen region is far away from the C-monomer so that the interaction between them has practically no effect on electronic structures of A. The active regions interact strongly with the C-monomers, therefore both B and C regions form the "interactive" regions.

(c) The eigenvalue problem is solved in the reduced space, i.e. in the interactive region (B + C) under the applied electric field. It should be stressed that in the elongation step, the frozen region is excluded from the variational space.

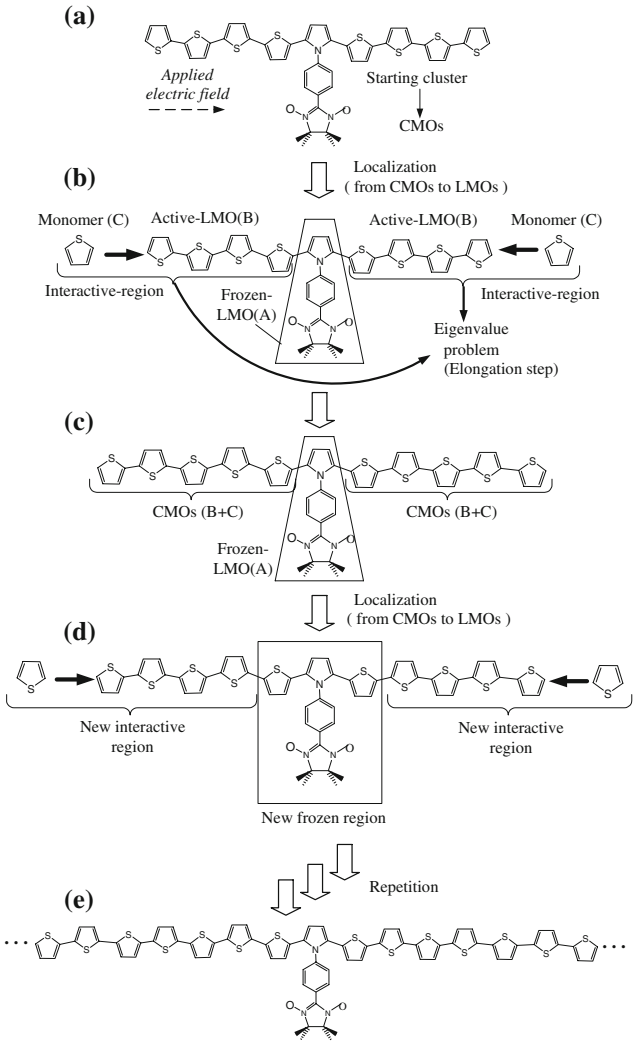

Fig. 2 The main steps of calculating the electronic structure of large aperiodic systems under an applied electric field within the elongation scheme. The static electric field parallel to the molecular wire is applied from left to right as shown in (**a**)

(d) In the next step, the frozen region is extended to the right and left from the SPD part by thiophene rings, i.e. new frozen region is now formed by SPD and two thiophene rings. As one may notice, the number of thiophene rings in active region remains unchanged. The eigenvalue problem is solved for a newly formed interactive region.

(e) By repeating localization and elongation steps, the electronic structure of large aperiodic systems such as spin-polarized molecular wire **1** can be obtained.

The methodology presented above guarantees computational efficiency due to substantial reduction of the size of the variational space. The size, i.e. the number of active space MOs is constant and relatively small. This simplification has only minor influence on the accuracy since the active space includes several units directly interacting with

attacking monomers. Therefore, the electronic structure of aperiodic polymer can be efficiently calculated with high accuracy. In this work, the elongation procedure has been implemented and linked to the GAMESS program package [60].

The electronic structure under the applied static electric field is calculated by adding the $\vec{\mu} \cdot \vec{E}$ term to the Hamiltonian, that is $H = -(1/2)\Delta + V(\vec{r}) + \vec{\mu} \cdot \vec{E}$, where $\vec{\mu}$ and $\vec{E}$ are the dipole moment operator and the electric field, respectively. The magnitude of the applied electric field is ranging from 0.0000 to 0.0020 a.u. The direction of the field is along the molecular wire. The remaining ab initio and semi-empirical MO calculations other than the elongation method were performed using Gaussian03 program package [61].

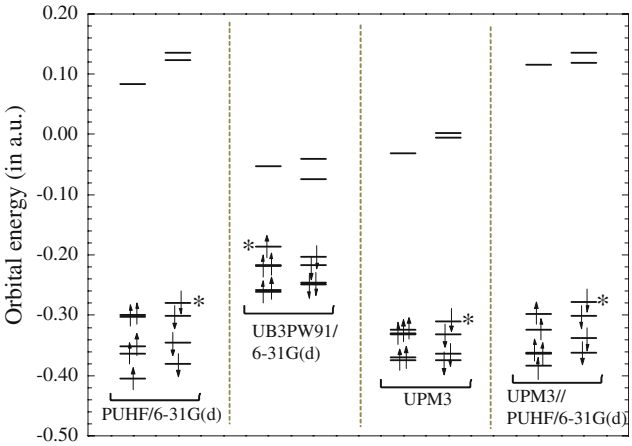

Fig. 3 Orbital energies of the pyrrole-based spin-polarized donor **2**. *Asterisk* indicates the highest occupied orbital

3 Results and discussion

3.1 Electronic structure of spin-polarized donor molecule

First, the electronic structure of the pyrrole-based SPD **2** was calculated at the spin-projected PUHF/6-31G(d), UB3PW91/6-31G(d), UPM3, and UPM3//PUHF/6-31G(d) levels. In the calculations, restricted geometry optimizations were performed by imposing planarity on system **2**. The UHF level of theory gives us direct reference to previous investigations on SPD systems [22, 25, 33–36]. Spin contamination effects cannot be eliminated completely, even by applying the spin-projected technique. For example, the $\langle s^2 \rangle$ value of SPD **2** was equal to 1.65 and 1.20 at the PUHF/6-31G(d) and UPM3//PUHF/6-31G(d) levels of theory, respectively, while the exact value should be equal to 0.75. The restricted-open Hartree–Fock (ROHF) treatment that does not suffer from spin contaminations, by definition, cannot be applied for describing spin polarization effects. Figure 3 shows MO energy diagram near SOMO in the pyrrole-based SPD **2**. It is found that the energy level of HOMO(β) is above that of SOMO(α) except for the UB3PW91/6-31G(d) level. Such a qualitative picture of orbital energy levels is also confirmed by fully optimized PUHF/6-31G(d) calculations. In other words, the electronic structure near SOMO does not strongly depend on the conformation. In unconstrained structure of **2**, the torsion angle between pyrrole and benzene rings is equal to 44.6°, while the angle between a benzene ring and a radical unit is equal to 7.2°. In contrast, density functional theory (DFT) calculations for SPD **2** at UB3PW91/6-31G(d) level predict that the highest occupied MO is an α-spin orbital (see Fig. 3). However, DFT level is not used for our purpose because orbital energies obtained from DFT calculations have no simple physical meaning as described in Ref. [62].

It is expected that the interaction between radical and donor units is responsible for very unique property of SPD; in which the orbital energy of HOMO(β) is higher than that of SOMO(α). In order to confirm this, we examined the MOs of SPD molecule **2** at the UPM3 level based on optimized PUHF/6-31G(d) geometry. The analysis is focused on the MO correlation diagrams between donor units, i.e. pyrrole and benzene rings, and radical unit, i.e. NN. The interaction profiles near SOMO are shown in Fig. 4. The MO diagrams for α- and β-spin orbitals are illustrated at left- and right-hand sides of the figure, respectively. Panel (a) illustrates the interaction between benzene ring and NN. It can be seen that the interaction between HOMO of benzene ring (A_1 symmetry) and HOMO of NN (A_1) gives new MOs ϕ^+ (in phase, $1A_1$) and ϕ^- (out of phase, $2A_1$) of phenyl NN for both α- and β-spin resolutions. The ϕ^+ is stabilized by the interaction, while the ϕ^- is destabilized. In the case of β-spin orbital, in particular, the orbital energy of ϕ^- was increased largely compared with that in the case of α-spin orbital. This difference between α- and β-spin orbitals is mainly due to the effect of spin polarization in NN, that is, HOMO(β) of NN has higher energy than HOMO(α) of NN does. The spin polarization effect causes small difference in orbital energy between the HOMO(β) of benzene ring and HOMO(β) of NN. In contrast, there is large difference between HOMO(α) of benzene ring and HOMO(α) of NN. Because of the strong interaction between HOMO(β) of benzene ring and HOMO(β) of NN, the order of orbital energies of phenyl NN becomes SOMO(α) > HOMO(β) > HOMO(α). Here we approximately considered only orbital energy difference. Figure 4b shows the correlation diagrams among pyrrole ring and phenyl NN molecular orbitals. The interaction between NHOMO of pyrrole ring (A_1) and HOMO of phenyl NN (A_1) leads to new MOs ϕ^+ (in phase, $1A_1$) and ϕ^- (out of phase, $2A_1$) of SPD molecule for both

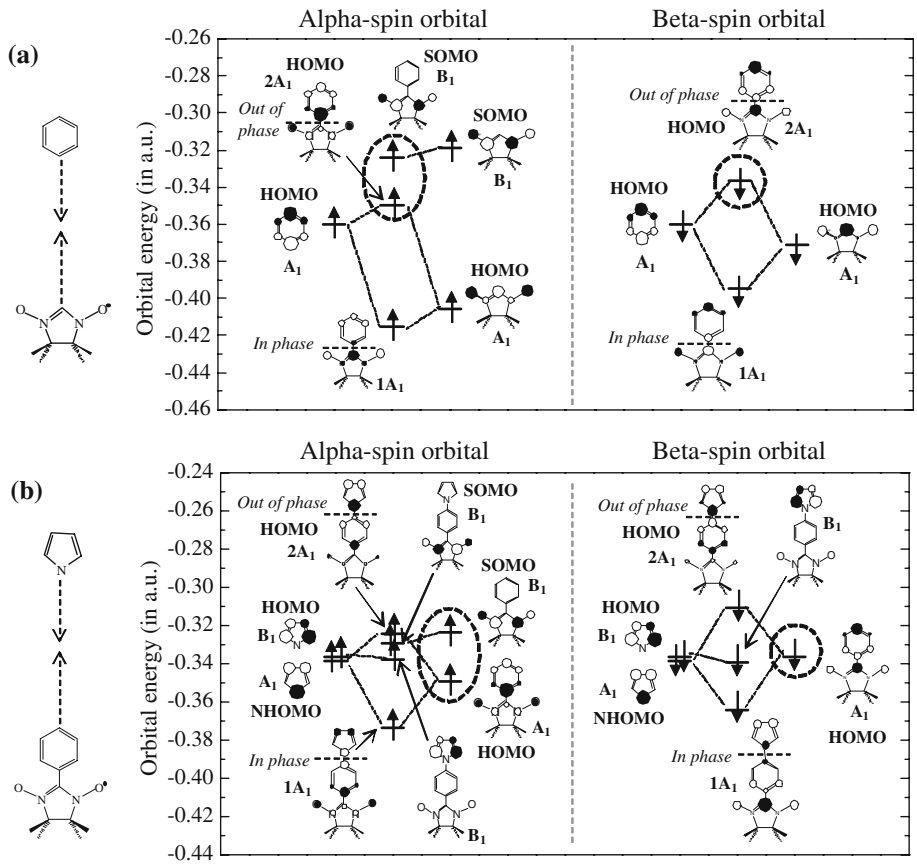

Fig. 4 The MO correlation diagrams for the pyrrole-based spin-polarized donor **2** (UPM3//PUHF/6-31G(d)); The *rows* (**a**) and (**b**), respectively, correspond to interactions of benzene ring with nitronyl nitroxide (*NN*) and those of pyrrole ring with phenyl NN. Only the p-orbitals perpendicular to the molecular plane are shown. The *left* and *right*-hand side diagrams correspond to α- and β-spin orbital resolutions, respectively. The notation of C_{2v} symmetry is adopted. In each spin orbital, *dotted circles* in (**a**) and (**b**) show the same orbital(s)

spin resolutions. Small difference in orbital energy was found between the NHOMO(β) of pyrrole ring and HOMO(β) of phenyl NN, while there is large difference between the NHOMO(α) of pyrrole ring and HOMO(α) of phenyl NN. In the similar manner to Fig. 4a, the strong interaction is expected between NHOMO(β) of pyrrole ring and HOMO(β) of phenyl NN. The interaction causes the important property of SPD molecule **2** that the β-spin orbital is higher than α-spin orbital, that is, the order of orbital energies of the SPD molecule becomes HOMO(β) > HOMO(α) > SOMO(α). In this way, the unique property of SPD molecule can be explained by the strong interaction between donor and radical units in the β-spin orbital.

3.2 Dependence of electronic structures on the length of spin-polarized molecular wire

The elongation calculations were performed to elucidate the electronic structure of the pyrrole-based spin polarized molecular wire **1** under an electric field. The geometry of spin-polarized molecular wire was obtained by the following steps:

(i) The structure of central SPD part was fully optimized at the PUHF/6-31G(d) level.

(ii) Penta-thiophene oligomer was optimized at the RHF/6-31G(d) level with a fixed planar structure. The geometry of thiophene unit was assumed to be equivalent to the central thiophene ring of the oligomer.

(iii) The SPD and wire parts are built by keeping the straight, planar shape of the molecular wire as shown in Fig. 1a.

In the steps (i) and (ii), the geometry optimizations were performed in the absence of external electric field. Of course, the field will have effect on the geometry and on the electronic structure of the system. However, this complication was not taken into account in the present study. The validity of the elongation method has been well documented in Refs. [47–59]. Here we examine the validity of the elongation method for spin-polarized molecular wires in the presence of an electric field. The total energy of the system was calculated at the UPM3 level. The static electric field $|\vec{E}| = 0.0010$ a.u. along the molecular wire was applied from left to the right (Fig. 2a). A comparison between elongation and conventional total energies for $N_{st} = 8 \rightarrow 28$ calculations confirms accuracy of the elongation method. Even in the last elongation step with 28 thiophene rings, the deviation in total energy from the conventional reference energy is about 5.5×10^{-6} a.u.

This is sufficiently accurate to analyze spin-polarized molecular wires under the applied electric field.

Next, we examine dependence of the electronic structure on the length of the molecular wire under the applied electric field. Figure 5a shows the relationship between the changes of net charges and the length of molecular wire with the electric field $|\vec{E}| = 0.0020$ a.u., where Mulliken charges are used for all the population analysis at the PM3 level. The difference in net charge from field "free" ($|\vec{E}| = 0.0000$ a.u.) calculations is analyzed. Here, we plotted the change in the net charge of each thiophene ring. The central SPD part corresponding to site-0 is excluded from the figure. A negative value indicated an increase in the electronic density. One can see from Fig. 5a that the electronic structure is mainly changed at both ends of molecular wire regardless of the length of the wire. The electron population increases on the left-hand side of the wire, while it decreases on the right-hand side. This electron transfer in the system is caused by the electric field applied from left to the right (left side corresponds to positive charge, right side corresponds to negative charge). In other words, the electrons of wire are attracted by the applied electric field, and flow from right side to left side, i.e., in the opposite direction to the applied electric field.

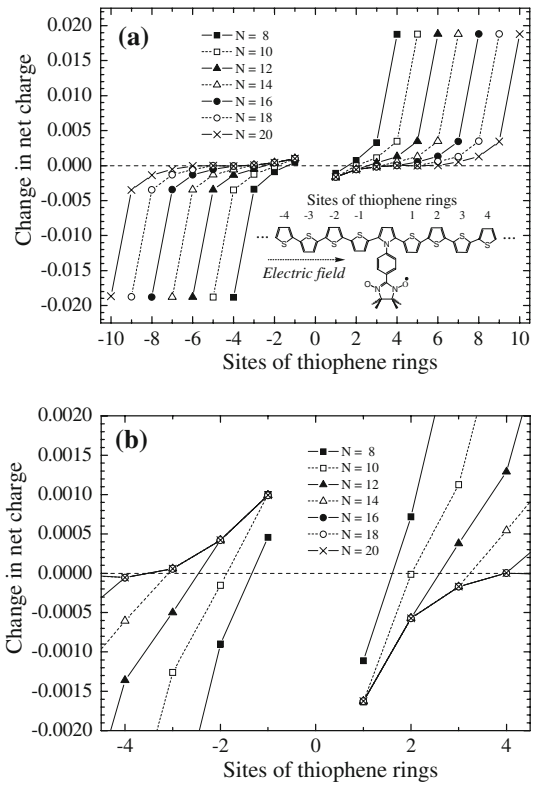

Fig. 5 Change in net charge of each thiophene ring by the applied electric field, $|\vec{E}| = 0.0020$ a.u. (UPM3). **a** General drawing, **b** enlarged view of the center part. *Graph* shows the difference in net charge from zero electric field ($|\vec{E}| = 0.0000$ a.u.). "*N*" is the number of thiophene rings. The sites of thiophene rings are depicted in (**a**)

Figure 5b shows the enlarged view of the central part of panel (a). In the central part of the system, the electron density decreases on the left-hand side of SPD-part, while it increases on the right-hand side of SPD-part. This means that the electrons in the central part flow in the same direction as the applied electric field, that is, from left to right side. This is the opposite behavior to the end part of the system as shown in panel (a). In addition, the increase of the electron population in the right side was larger than the decrease in the left side. Such tendencies observed in charge reorganization in the central part converged for at least 14 thiophene rings in the system. Therefore, for simplicity, subsequent analyses were performed using the spin-polarized molecular wire with 14 thiophene rings. In the next subsection, we will discuss the behavior of the net charges of the central part of the system.

3.3 Delocalization of β-spin electrons in spin-polarized molecular wire by the applied electric field

What is responsible for the unique behavior of the electrons in the center of the system composed of SPD and 14 thiophene rings? To explain this behavior, we examined the role of each part of the SPD, namely pyrrole ring, benzene ring, and NN. Figure 1d shows additional model molecules, introduced for analyzing the pyrrole-based spin-polarized molecular wire **1**. In model **3**, we simply disregard the radical unit, i.e., NN. The benzene ring is neglected in model **4**. The donor unit is excluded in model **5**, that is, the pyrrole ring is replaced by a thiophene ring. In the molecules **1**, **3**–**5**, the system is divided into "SPD part" and "wire part" as shown in Fig. 1a and d. The molecular "wire part" in **1**, **3**–**5** is composed of 14 thiophene rings. Thus, the resulting oligo-thiophene **5** includes 15 thiophene rings; a central thiophene ring constitutes the SPD part and the remaining 14 thiophene rings are in the wire part in **5**. We further define "net charge of SPD part" and "net charge of wire part" by summing the net charges of SPD part and those of the wire part, respectively.

Figure 6a shows the relationship between the strength of the applied electric field and the change in the net charge of wire part. The negative value of the change in net charge of wire part indicates that the wire part obtains extra electrons from the SPD part. As seen from the figure, there is no delocalization of electrons from the SPD part to wire part in model **5**. The change in the net charge of wire part is practically equals to zero regardless of the strength of the applied electric field. One should expect such behavior, because the SPD and wire parts are built from the same thiophene ring. In model **4**, the net charge of wire part decreases with the increase in the strength of the applied

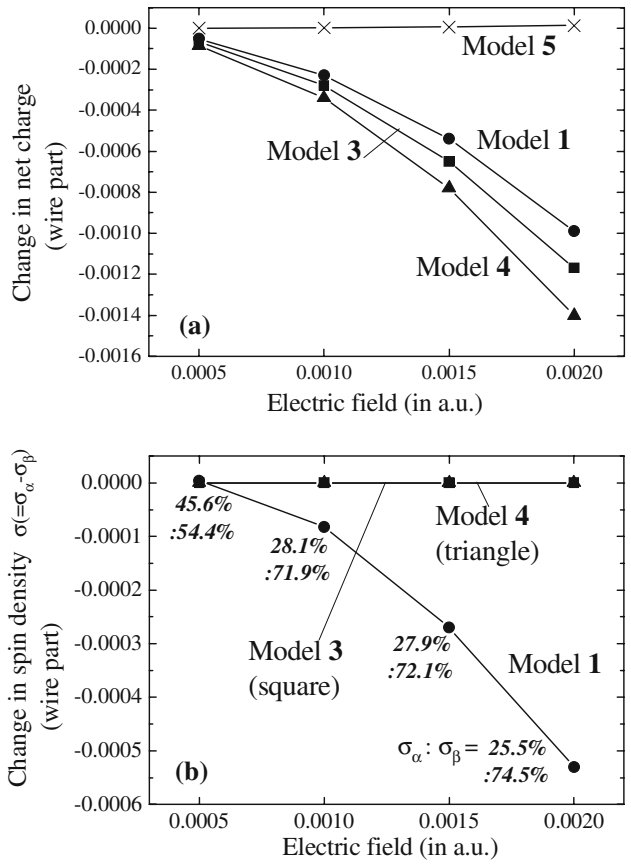

Fig. 6 Change in (**a**) net charge and (**b**) spin density σ ($=\sigma_\alpha - \sigma_\beta$) of wire part under the applied electric field for the models **1**, **3**–**5** (UPM3) with respect to field free ($|\vec{E}| = 0.0000$ a.u.) case. The ratio of α- and β-spin densities (σ_α:σ_β) for model **1** is shown next to the plot in (**b**)

electric field. The replacement of the thiophene ring by the pyrrole ring leads to a charge accumulation in the wire. The wire part obtained about 0.0014 electrons under the applied electric field $|\vec{E}| = 0.0020$ a.u. In other words, the electrons of the central pyrrole ring flow into the wire part. In models **1** and **3**, the tendency of charge accumulation in the wire part is similar to that in model **4** but to a lesser amount. Therefore, the pyrrole ring plays a dominant role in delocalizing the electrons from the SPD part to the wire part.

Now, we examine the spin density (σ) which is defined as the difference between α-spin density (σ_α) and β-spin density (σ_β), that is, $\sigma = \sigma_\alpha - \sigma_\beta$. Figure 6b shows the change in spin density σ under the applied electric field for the wire part of models **1**, **3**, and **4** in which the delocalization of electrons was observed. The spin density of the wire part decreases as the strength of the applied electric field increases in model **1**. When the applied electric field is set to $|\vec{E}| = 0.0020$ a.u., the change in spin density is about -0.0005. That is to say, β-spin density is larger than α-spin density by 0.0005 in the wire part. These results mean that the flow of β-spin electrons from the central SPD part to the wire part is 0.0005 more than that of α-spin electrons. In addition, we find that 74.5% of the delocalized electrons under the applied electric field $|\vec{E}| = 0.0020$ a.u. possess β-spin. The percentage of β-spin density increases with increasing magnitude of the electric field. In models **3** and **4** there is no radical unit, therefore, the spin density does not change by the applied electric field. It is not surprising since both models are closed-shell systems; UHF results for closed-shell systems are practically equivalent to RHF results. Therefore, the spin-dependent delocalization of electrons over the molecular wire should be only expected for model **1**.

Finally, we have to inquire, "where are the delocalized electrons?" Fig. 7 shows the change in the net charge at each thiophene ring for models **1**, **3**–**5** under various applied electric fields of $|\vec{E}| = 0.0005$, 0.0010, 0.0015, and 0.0020 a.u. In this graph, we traced the central part of the system. There is no change in charge distribution for model **5** regardless of the applied electric field (panel (d)). In model **4** (panel (c)), the electrons of the SPD part are delocalized over one or two thiophene rings next to the central pyrrole ring, and this tendency is strengthened with intensity of the applied electric field. Model **3** in panel (b) exhibits the similar tendency to model **4**. Thus, the benzene ring added to the SPD part plays a role of a spacer here. Model **1** in panel (a) shows quite different behavior from the other models. On the right hand side of the SPD part, the electron population increases with increasing magnitude of the electric field, whereas on the left hand side of the SPD part, the electron population decreases. This result means that the NN as a radical unit can shift the distribution of electrons in the same direction as the applied electric field, that is, from left side to right side of the graph. Furthermore, β-spin electrons are dominant components in the spin-distribution of the localized electrons in model **1**, as mentioned above. In contrast, α- and β-electrons are distributed equally on the wire part in the other models. Therefore, the radical unit of model **1** is responsible for the spin-distribution on the molecular wire.

4 Conclusions

In the present article, we have analyzed the electronic structure of pyrrole-based spin-polarized molecular wire under an applied electric field. We come to the following conclusions for the spin-polarized molecular wire. The unique feature of the SPD that the HOMO(β) is higher than SOMO(α) is confirmed by semi-empirical and ab initio MO calculations. This feature can be explained by the strong interaction between donor and radical units in the β-spin orbital. Pyrrole-based spin-polarized molecular wire was analyzed in the presence of an electric field by the

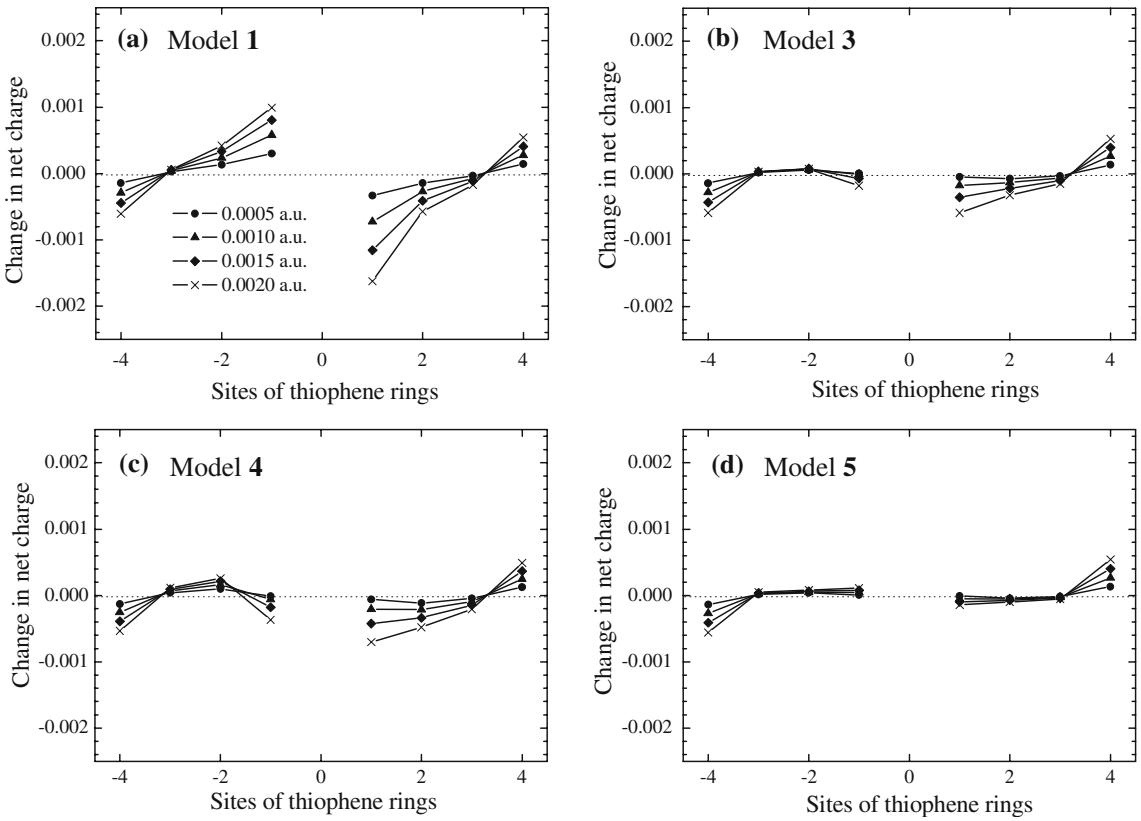

Fig. 7 Dependence of net charge on the applied electric field for models **1**, **3–5** (UPM3). *Graph* shows the enlarged view of central part of the system. Each *plot* indicates the difference from field free ($|\vec{E}| = 0.0000$ a.u.) case. The sites of thiophene rings are depicted in Fig. 5a

elongation method. It was found that the pyrrole ring in the SPD part triggers off delocalization of electrons over the thiophene rings next to the SPD part. In addition, the NN radical unit shows two important properties. First, it changes the spin-distribution from same ratio of α- and β-spins to dominant β-spin. Second, it shifts the distribution of electrons in the same direction as the applied electric field.

We hope that these results provide a novel insight into the investigation of spin-polarized molecular wires under the influence of applied electric fields, and help in the design of molecular quantum spin devices.

Acknowledgments This work was supported by a grant-in-aid from the Ministry of Education, Culture, Sports, Science and Technology (MEXT) of Japan (No 19350012) and Group, PRESTO, Japan Science and Technology Agency (JST). The calculations were performed on the Linux PC clusters in our laboratory.

References

1. Prinz GA (1998) Science 282:1660
2. Tsukagoshi K, Alphenaar BW, Ago H (1999) Nature 401:572
3. Johnson M (2000) IEEE Spectrum 37:33
4. Zhang P, Xue Q-K, Wang Y, Xie XC (2002) Phys Rev Lett 89:286803
5. Petta JR, Slater SK, Ralph DC (2004) Phys Rev Lett 93:136601
6. Liu R, Ke S-H, Baranger HU, Yang W (2005) Nano Lett 5:1959
7. Morten JP, Brataas A, Belzig W (2005) Phys Rev B 72:014510
8. de Groot RA, Mueller FM, van Engen PG, Buschow KHJ (1983) Phys Rev Lett 50:2024 For example
9. Rajca A (1994) Chem Rev 94:871
10. Miller JS, Epstein AJ (1994) Angew Chem Int Ed Engl 33:385
11. Aoki Y, Imamura A (1999) Int J Quantum Chem 74:491
12. Pranata J (1992) J Am Chem Soc 114:10537
13. Mitani M, Mori H, Takano Y, Yamaki D, Yoshioka Y, Yamaguchi K (2000) J Chem Phys 113:4035
14. Matsuda K, Irie M (2000) J Am Chem Soc 122:7195
15. Teki Y, Miyamoto S, Iimura K, Nakatsuji M, Miura Y (2000) J Am Chem Soc 122:984
16. Teki Y, Miyamoto S, Nakatsuji M, Miura Y (2001) J Am Chem Soc 123:294
17. Rajca A, Wongsriratanakul J, Rajca S (2001) Science 294:1503
18. Huai P, Shimoi Y, Abe S (2003) Phys Rev Lett 90:207203
19. Dias JR (2003) J Chem Inf Comput Sci 43:1494
20. Rajca A, Wongsriratanakul J, Rajca S (2004) J Am Chem Soc 126:6608
21. Rajca S, Rajca A, Wongsriratanakul J, Butler P, Choi S (2004) J Am Chem Soc 126:6972
22. Izuoka A, Hiraishi M, Abe T, Sugawara T, Sato K, Takui T (2000) J Am Chem Soc 122:3234
23. Teki Y (2005) Polyhedron 24:2299
24. Matsushita MM, Kawakami H, Okabe E, Kouka H, Kawada Y, Sugawara T (2005) Polyhedron 24:2870
25. Nakazaki J, Chung I, Watanabe R, Ishitsuka T, Kawada Y, Matsushita MM, Sugawara T (2003) Internet Electron J Mol Design 2:112

26. Minamoto M, Matsushita MM, Sugawara T (2005) Polyhedron 24:2263
27. Nickels P, Matsushita MM, Minamoto M, Komiyama S, Sugawara T (2008) Small 4:471
28. Sugawara T, Minamoto M, Matsushita MM, Nickels P, Komiyama S (2008) Phys Rev B 77:235316
29. Ito A, Urabe M, Tanaka K (2003) Polyhedron 22:1829
30. Nakazaki J, Matsushita MM, Izuoka A, Sugawara T (1997) Mol Cryst Liq Cryst 306:81
31. Sugawara T (1999) Mol Cryst Liq Cryst 334:257
32. Nakazaki J, Matsushita MM, Izuoka A, Sugawara T (1999) Tetrahedron Lett 40:5027
33. Yamaguchi K, Okumura M, Nakano M (1992) Chem Phys Lett 191:237
34. Sakurai H, Izuoka A, Sugawara T (2000) J Am Chem Soc 122:9723
35. Nakazaki J, Ishikawa Y, Izuoka A, Sugawara T, Kawada Y (2000) Chem Phys Lett 319:385
36. Nakazaki J, Chung I, Matsushita MM, Sugawara T, Watanabe R, Izuoka A, Kawada Y (2003) J Mater Chem 13:1011
37. Matsushita MM, Kawakami H, Kawada Y, Sugawara T (2007) Chem Lett 36:110
38. Matsushita MM, Kawakami H, Sugawara T, Ogata M (2008) Phys Rev B 77:195208
39. Emberly EG, Kirczenow G (2002) Chem Phys 281:311
40. Pati R, Senapati L, Ajayan PM, Nayak SK (2003) Phys Rev B 68:100407
41. García JCS, Horowitz G, Brédas JL, Cornil J (2003) J Chem Phys 119:12563
42. Jalili S, Tabar HR (2005) Phys Rev B 71:165410
43. Viljas JK, Pauly F, Cuevas JC (2008) Phys Rev B 77:155119
44. Evans JS, Cheng C-L, Voorhis TV (2008) Phys Rev B 78:165108
45. Zhou L, Yang S-W, Ng M-F, Sullivan MB, Tan VBC, Shen L (2008) J Am Chem Soc 130:4023
46. Wang L, Cai Z, Wang J, Lu J, Luo G, Lai L, Zhou J, Qin R, Gao Z, Yu D, Li G, Mei WN, Sanvito S (2008) Nano Lett 8:3640
47. Imamura A, Aoki Y, Maekawa K (1991) J Chem Phys 95:5419
48. Gu FL, Aoki Y, Imamura A, Bishop DM, Kirtman B (2003) Mol Phys 101:1487
49. Ohnishi S, Gu FL, Naka K, Imamura A, Kirtman B, Aoki Y (2004) J Phys Chem A 108:8478
50. Gu FL, Aoki Y, Korchowiec J, Imamura A, Kirtman B (2004) J Chem Phys 121:10385
51. Aoki Y, Gu FL, Korchowiec J, Imamura A, JST (2008) Japan Patent No. 4221351, 21 Nov 2008
52. Korchowiec J, Gu FL, Imamura A, Kirtman B, Aoki Y (2005) Int J Quantum Chem 102:785
53. Korchowiec J, Gu FL, Aoki Y (2005) Int J Quantum Chem 105:875
54. Makowski M, Korchowiec J, Gu FL, Aoki Y (2006) J Comp Chem 27:1603
55. Gu FL, Imamura A, Aoki Y (2006) Elongation method for polymers and its application to nonlinear optics, in atoms, molecules and clusters in electric fields: theoretical approaches to the calculation of electric polarizabilities. In: Maroulis G (ed) Imperial College Press, vol 1, pp 97–177
56. Orimoto Y, Gu FL, Imamura A, Aoki Y (2007) J Chem Phys 126:215104
57. Ohnishi S, Orimoto Y, Gu FL, Aoki Y (2007) J Chem Phys 127:084702
58. Zhang R, Tian WQ, Gu FL, Aoki Y (2007) J Phys Chem C 111:6350
59. Räther G, Aoki Y, Imamura A (1999) Int J Quantum Chem 74:35
60. GAMESS, Schmidt MW, Baldridge KK, Boatz JA, Elbert ST, Gordon MS, Jensen JH, Koseki S, Matsunaga N, Nguyen KA, Su SJ, Windus TL, Dupuis M, Montgomery JA (1993) J Comput Chem 14:1347
61. Gaussian 03, Revision C.02, Frisch MJ, Trucks GW, Schlegel HB, Scuseria GE, Robb MA, Cheeseman JR, Montgomery JA Jr, Vreven T, Kudin KN, Burant JC, Millam JM, Iyengar SS, Tomasi J, Barone V, Mennucci B, Cossi M, Scalmani G, Rega N, Petersson GA, Nakatsuji H, Hada M, Ehara M, Toyota K, Fukuda R, Hasegawa J, Ishida M, Nakajima T, Honda Y, Kitao O, Nakai H, Klene, Li X, Knox JE, Hratchian HP, Cross JB, Adamo C, Jaramillo J, Gomperts R, Stratmann RE, Yazyev O, Austin AJ, Cammi R, Pomelli C, Ochterski JW, Ayala PY, Morokuma K, Voth GA, Salvador P, Dannenberg JJ, Zakrzewski VG, Dapprich S, Daniels AD, Strain MC, Farkas O, Malick DK, Rabuck AD, Raghavachari K, Foresman JB, Ortiz JV, Cui Q, Baboul AG, Clifford S, Cioslowski J, Stefanov BB, Liu G, Liashenko A, Piskorz P, Komaromi I, Martin RL, Fox DJ, Keith T, Al-Laham MA, Peng CY, Nanayakkara A, Challacombe M, Gill PMW, Johnson B, Chen W, Wong MW, Gonzalez C, Pople JA, Gaussian, Inc., Wallingford, CT, 2004
62. Parr RG, Yang W (1989) International series of monographs on chemistry 16: density-functional theory of atoms and molecules. Oxford University Press, New York, pp 142–168